

RSC Advances



This is an *Accepted Manuscript*, which has been through the Royal Society of Chemistry peer review process and has been accepted for publication.

Accepted Manuscripts are published online shortly after acceptance, before technical editing, formatting and proof reading. Using this free service, authors can make their results available to the community, in citable form, before we publish the edited article. This *Accepted Manuscript* will be replaced by the edited, formatted and paginated article as soon as this is available.

You can find more information about *Accepted Manuscripts* in the [Information for Authors](#).

Please note that technical editing may introduce minor changes to the text and/or graphics, which may alter content. The journal's standard [Terms & Conditions](#) and the [Ethical guidelines](#) still apply. In no event shall the Royal Society of Chemistry be held responsible for any errors or omissions in this *Accepted Manuscript* or any consequences arising from the use of any information it contains.



Journal Name

Article

Atmospheric reactivity of HC≡CCH₂OH (2-propyn-1-ol) toward OH radical: Experimental determination and theoretical comparison with its alkyne analogue

Cite this: DOI: 10.1039/x0xx00000x

Received 00th January 2012,
Accepted 00th January 2012

DOI: 10.1039/x0xx00000x

www.rsc.org/

Rodrigo G. Gibilisco^a, Martina Kieninger^b, Oscar N. Ventura^b, and Mariano A. Teruel^{a*}^a INFIQC (CONICET- Facultad de Ciencias Químicas, Universidad Nacional de Córdoba). Dpto. de Físicoquímica, Ciudad Universitaria, 5000 Córdoba, Argentina.^b CCBG, DETEMA, Facultad de Química, Universidad de la República, CC1157, 11400 Montevideo, Uruguay.* Corresponding author: Mariano A. Teruel (mteruel@fcq.unc.edu.ar)

The rate coefficient for the reaction of propargyl alcohol (2-Propyn-1-ol, 2P1OL) with OH radicals has been determined using gas chromatography with a flame ionization detector (GC/FID) at 298 K and atmospheric pressure. The experimental value obtained by the relative method using methyl methacrylate and butyl acrylate as references was $(2.05 \pm 0.30) \times 10^{-11} \text{ cm}^3 \text{ molecule}^{-1} \text{ s}^{-1}$. The present value was compared with previous determinations and a theoretical study of the reaction was performed in order to explain the differences on reactivity of the alcohol with that of the corresponding alkyne (propyne, P). A full discussion of the addition and abstraction mechanisms was developed for 2P1OL at the density functional and *ab initio* composite model levels. It was found that addition is much faster than abstraction for propyne but occur at approximately the same rate for 2P1OL. In this last case, however, abstraction of hydrogen from the C1 carbon leads to a complex which can react further to yield addition products. Thermodynamic and kinetic data calculated for these reactions suggest that the products would be the 1,2- and 1,3-propenol radicals. These products would react further with O₂, in case it is present in the reaction mixture.

Introduction

In the framework of the studies of OH-initiated degradation of oxygenated volatile organic compounds (OVOCs) emitted by industrial activity or by vegetation, it is important to determine the fate and lifetime of OVOCs in the lower troposphere [1].

Alkynes are atmospherically important species since dicarbonyl compounds generated by their OH-initiated oxidation react rapidly with oxygen to give organic acids [2], which contribute to acid rain. Propargyl alcohol (2-Propyn-1-ol, 2P1OL) is widely used as corrosion inhibitor in solutions of metal complexes [3-5]. It is also used as intermediate in organic synthesis and as solvent and stabilizing additive in electroplating rinsing for the manufacture of mirrors.

In the atmosphere, reaction of alkynes with OH radicals proceeds mainly by addition to the C-C triple bond; however there is a small contribution of the hydrogen abstraction channel when allowed [6]. The stability of the alkoxy radical formed depends on the chain length and the possibilities of stabilization of the electronically excited adduct, which could minimize decomposition to initial reactants [6-8].

While there are several studies concerning the degradation of unsaturated alcohols initiated by the main tropospheric oxidants [9-12], information on the reactions of alkynols is still scarce [13, 14]. A relative kinetic study of the reaction of OH + 3,5-dimethyl-1-hexin-3-ol in 1 atm of air in the presence of NO_x was reported in the literature, and there is also an absolute determination of the rate coefficient of the reaction OH + 2P1OL at low pressures (1.33 to 2.67 kPa) using pulsed

laser photolysis coupled with laser induced fluorescence technique (PLP-LIF). In this latter study, the authors evaluated also the possibility of formation of different adducts depending on the position of the OH radical attack to the C-C triple bond. A theoretical study of the degradation mechanism of the reaction of propargyl alcohol initiated by the OH radical has been also reported. This study gave more evidence of the importance of atmospheric oxidation of alkynes as a result of the formation of dicarbonyl compounds and acids in their reaction with molecular oxygen [15].

Calvert *et al.* [16] have suggested that the value obtained by Upadhaya *et al.* for OH + 2P1OL at low pressure is not applicable to atmospheric conditions, and tentatively ascribed those results to a pressure dependence of the rate coefficient like in the reaction of allyl alcohol + OH radicals [13]. In that case, they obtained a lower rate coefficient of k(OH + allyl alcohol) than in previous studies conducted near atmospheric pressure [17-19]. Consequently, Calvert *et al.* recommended further work to determine the rate coefficient of 2P1OL + OH reaction at atmospheric pressure [16].

In this context, and given the necessity to have kinetic and mechanistic information at atmospheric conditions, we present in this work the rate constant for the atmospheric oxidation of 2P1OL initiated by OH radicals at 1 atm and 298 K to determine the difference, if any, with the data of Upadhaya *et al.* at different pressures [14].

Additionally, a theoretical investigation of the reaction of OH radicals with 2-propin-1-ol (2P1OL) and propyne (P) was developed to elucidate the differences in reactivity of 2P1OL and the analog alkyne at different temperatures:



The goal of the present work was to find an explanation that the rate of reaction (1) determined in our work is more than two times larger than the rate coefficient of reaction (2) determined by Atkinson and Aschmann, $(6.21 \pm 0.31) \times 10^{-12} \text{ cm}^3 \text{ molecule}^{-1} \text{ s}^{-1}$ [20]. In this paper, addition of OH to different sites was studied: C2 and C3 for 2P1OL and C1 and C2 for P. In the case of 2P1OL, the abstraction of the hydroxyl hydrogen has also been studied in order to have a full appraisal of the possible mechanisms.

2. Materials and Methods

2.1 Experimental Procedures

The experimental set-up consisted of an 80 L Teflon bag located in a wooden box with the internal walls covered with aluminum foil, and operated at atmospheric pressure (100.0 \pm 1.3 kPa) and (298 \pm 1)K. The temperature of the reactor and photolysis chamber were in equilibrium with the surroundings where temperature variation recorded was never higher than

\pm 5 K. No significant variation of the kinetic results were observed in this temperature range.

Measured amounts of the organic reactants were flushed into the bag with a stream of nitrogen. The bag was then filled to its full capacity at atmospheric pressure with nitrogen. H₂O₂ was used to generate OH radicals by photolysis using a set of germicidal lamps:

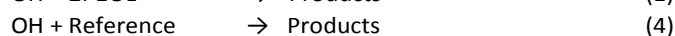


These lamps provide UV-radiation with a λ maximum around 254 nm. In the present work, typically 6 of these lamps were used to produce OH radicals and the time of photolysis varied from 2 to 5 minutes.

Reaction mixtures consisting of a reference organic compound and the sample organic reactant, diluted in nitrogen, were prepared in the reaction chamber and left to mix, prior to photolysis, for approximately 1 h. Before each set of experiments, the bag was cleaned by filling it with a mixture of O₂ and N₂ photolyzed for 15-25 min using 4 germicidal lamps (Philips 30W) with a UV emission at 254 nm, to produce O₃. After this procedure, the bag was cleaned up again by repeated flushing with air and the absence of impurities was checked by gas chromatography before performing the experiments.

Gas samples were periodically removed from the Teflon bag using a gas tight syringe and put into the injector port at 473 K. Organics were monitored by gas chromatography (Shimadzu GC-14B) coupled with flame ionization detection (FID), using a HP-20 capillary column held from 313 to 393 K.

In the presence of the oxidant OH radical the alcohol studied and the references decay through the following reactions:



Provided that the reference compound and the alcohol are lost only by reactions (1) and (4), then it can be shown that:

$$\ln\{[2\text{P1OL}]_0/[2\text{P1OL}]_t\} = (k_1/k_4) \ln\{[\text{Ref}]_0/[\text{Ref}]_t\} \quad (I)$$

where [2P1OL]₀, [Ref]₀, [2P1OL]_t and [Ref]_t are the concentrations of the alcohol and the reference compound at times t=0 and t, respectively, and k₁ and k₄ are the rate constants of reactions (1) and (4), respectively.

The relative rate technique relies on the assumption that the alcohol and the reference compounds are removed solely by reaction with OH radicals. To verify this assumption, mixtures of hydrogen peroxide and air with the alcohol of interest and the reference compound were prepared and allowed to stand in the dark for two hours. In all cases, the reaction of the organic species with the OH precursor (hydrogen peroxide), in

the absence of UV light, was of negligible importance over the typical time periods used in this work.

Furthermore, to test for possible photolysis of the reactants used, mixtures of the alcohols in air, in the absence of hydrogen peroxide, were irradiated for 30 minutes using the output of all the germicidal lamps surrounding the chamber. No significant photolysis of any of the reactants was observed. The initial concentrations used in the experiments were in the range of 70-200 ppm for 2P1OL, 80-250 ppm for methyl methacrylate and butyl acrylate.

2.2 Theoretical Methods

Theoretical calculations were performed using density functional methods (DFT) and composite quantum chemistry models of the Gaussian-n type (Gn). In particular, the M06 hybrid meta exchange-correlation DFT method of Zhao and Truhlar [21] and the BMK method of Boese and Martin [22] were used. Both DFT methods are especially tailored for thermodynamics, while the second is also adapted for kinetic calculations (the latter is more resource demanding than the former since it includes the kinetic density operator in the formula for the calculation of the exchange-correlation potential). In this work we used a valence triple zeta Pople basis set, augmented with diffuse functions in all atoms and including up to *f* polarization functions in the main atoms and *d* functions on the hydrogen atoms, 6-311++G(2df,2pd). This is a more extended and complete basis set than those used in similar studies [23], roughly in between aug-cc-pVTZ and aug-cc-pVQZ in Dunning's nomenclature [24]. The presence of *sp* diffuse functions helps to describe the more diffuse electron density of the radicals, as compared to that of closed-shell species, especially in the transition states. In addition to the DFT methods, the composite chemical models G2 and G4 have been employed. These models are based on *ab initio* calculations where different methods and basis sets with increased levels of accuracy are used to approach in a systematic way the accurate energy of the species. High level (i.e. QCISD(T) or CCSD(T)) correlation calculations with a moderate basis set are combined with energies from lower level calculations (MP4 or MP2) on optimized geometries at a generally correct level. Additionally, several molecule-independent empirical parameters (higher level correction (HLC) terms) are included to estimate remaining deficiencies of the calculations, under the assumption that they are systematic. The result is a very good approximation to the exact energy of the species in the non-relativistic limit. The G2 [25] and G4 [26] models differ in the complexity of the methods employed and the accuracy obtained. Although, both models are within chemical accuracy (i.e., errors smaller than 2 kcal/mol) the G4 method is more accurate (about 1. kcal/mol) but consequently more demanding from the point of view of time and resources needed.

In all cases studied, full geometry optimization of the structures was performed up to 10^{-4} Å accuracy in the Cartesian coordinates, with the aim of identifying all minima and transition states. Analytical second derivatives were used to calculate vibrational frequencies, which, in turn, were employed to guarantee the character of the critical point (either minimum or transition state) and to calculate thermodynamic properties using the standard statistical thermodynamics rigid rotor, harmonic oscillator, ideal gas model. The internal rotation of the OH group was not considered as a vibration, but the hindered rotor model was used instead. Results are reported at temperatures of 0 and 298 K, in both cases at the standard pressure of 101.325 kPa. The Gaussian 09 computer code [27] running in a mixed Xeon/Opteron cluster with 24 nodes/calculation was employed for this work. Theoretical methods referred above were used to study the structure of reactants, intermediates (pre-barrier complexes), transition states and products for the reactions.

2.3 Materials

The following chemicals with purities as stated by the supplier were used without further purification: nitrogen (AGA, 99.999%), 2P1OL (Aldrich, 98%), methyl methacrylate (Aldrich, 99.99%), butyl acrylate (Aldrich, 96%), and H₂O₂ (Cicarelli, 60% wt).

3. Results and Discussion

3.1. Relative rate measurements

Relative rate coefficient for the reactions of OH radicals with 2P1OL were determined by comparing the OH reaction with the alcohol studied to that with the reference compounds from equation (I). The data were fitted to a straight line by the linear least-squares procedure.

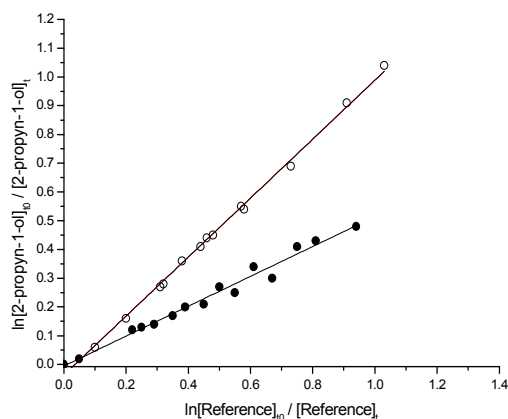


Figure 1: Relative rate data for the OH reaction with 2P1OL using methyl methacrylate (●) and butyl acrylate (o) as references compounds at 298 K and atmospheric pressure

Losses of 2P1OL by OH radicals are shown with different reference compounds in Figure 1.

The following were used as reference reactions to determine the rate coefficients of reaction (1):



where $k_6 = (4.15 \pm 0.32) \times 10^{-11} \text{ cm}^3 \text{ molecule}^{-1} \text{ s}^{-1}$ [28] and $k_7 = (1.80 \pm 0.26) \times 10^{-11} \text{ cm}^3 \text{ molecule}^{-1} \text{ s}^{-1}$ [29]. Table 1 shows the data on relative rate coefficients $k_{2\text{P1OL}}/k_{\text{Ref}}$ and absolute rate coefficients $k_{2\text{P1OL}}$ at room temperature (298 K). Ratios were obtained from the average of four experiments using different initial concentrations of 2P1OL. The rate coefficient obtained by averaging the values from different experiments was:

$$k_1 = (2.05 \pm 0.30) \times 10^{-11} \text{ cm}^3 \text{ molecule}^{-1} \text{ s}^{-1}$$

The error included in this value was calculated as twice the standard deviation arising from linear least-squares fit, and includes the corresponding errors in the reference rate coefficients of reactions (6) and (7). The linearity of the data points and the fact that the plots show practically no intercepts suggest that the contribution of secondary reactions with the products of the reactions studied here was negligible. Furthermore, in the present work we obtained two values of $k_{2\text{P1OL}}$ using two different reference compounds ($\text{CH}_2=\text{C}(\text{CH}_3)\text{C}(\text{O})\text{OCH}_3$ and $\text{CH}_2=\text{CHC}(\text{O})\text{O}(\text{CH}_2)_3\text{CH}_3$) and for each reactant organic studied, several runs were performed at different reference and alcohol concentrations, and different conversion yields. In all cases indistinguishable results were obtained from successive experiments.

Compound	Reference	$k_{2\text{P1OL}}/k_{\text{reference}}$	$k_{2\text{P1OL}}$ $10^{-11} \text{ cm}^3 \text{ molecule}^{-1} \text{ s}^{-1}$
2P1OL	Methyl methacrylate	0.51 ± 0.03	2.10 ± 0.15
	Methyl methacrylate	0.57 ± 0.01	2.40 ± 0.20
CH≡C-CH ₂ OH	Butyl acrylate	1.02 ± 0.02	1.80 ± 0.30
	Butyl acrylate	0.59 ± 0.03	1.90 ± 0.30
Average			2.05 ± 0.30

Table 1. Reference compound, measured rate coefficient ratios, $k_{\text{OVOC}}/k_{\text{Ref}}$, and the obtained rate coefficients for the reactions of OH radicals with 2P1OL at 298 K in 101.3 kPa of nitrogen.

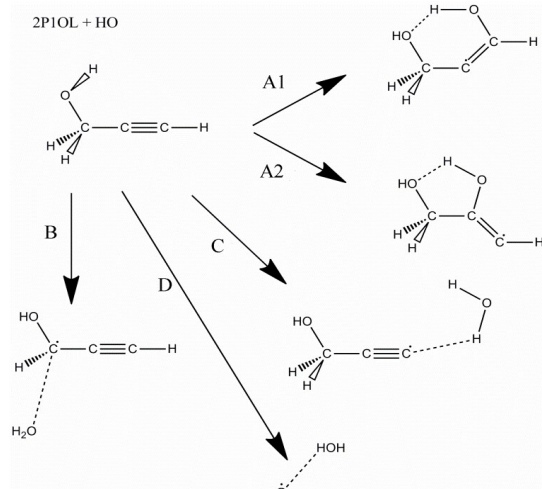
3.2. Comparison with previous experimental determinations

In previous kinetic determinations, Upadhyaya *et al.* [14] found a value of $k = (9.2 \pm 1.4) \times 10^{-12} \text{ cm}^3 \text{ molecule}^{-1} \text{ s}^{-1}$ in a

range of 1.33–2.67 kPa of total pressure of He by using the PLP-LIF technique. This value is lower than the rate coefficient obtained in our work of $k = (2.05 \pm 0.30) \times 10^{-11} \text{ cm}^3 \text{ molecule}^{-1} \text{ s}^{-1}$. The same trend was observed comparing the value of k determined by the same authors for the OH + propenol reaction, $k = (3.7 \pm 0.5) \times 10^{-11} \text{ cm}^3 \text{ molecule}^{-1} \text{ s}^{-1}$, about 40% lower than the values obtained by Papagni *et al.*, $k = (5.5 \pm 0.2) \times 10^{-11} \text{ cm}^3 \text{ molecule}^{-1} \text{ s}^{-1}$ [17], Orlando *et al.*, $k = (5.0 \pm 0.7) \times 10^{-11} \text{ cm}^3 \text{ molecule}^{-1} \text{ s}^{-1}$ [18], and Le Person *et al.* $k = (5.1 \pm 0.4) \times 10^{-11} \text{ cm}^3 \text{ molecule}^{-1} \text{ s}^{-1}$ [19]. These discrepancies are probably due to the experimental conditions used by Upadhyaya *et al.* [14] where k had not reached the high-pressure limit ($P \leq 2.67 \text{ kPa}$), as suggested by Calvert *et al.* [16]. Hence, the rate coefficient for the reaction of 2P1OL with OH radicals obtained in this work at standard conditions (298.15 K and 101.325 kPa), $k = (2.05 \pm 0.30) \times 10^{-11} \text{ cm}^3 \text{ molecule}^{-1} \text{ s}^{-1}$, can be adopted as the recommended value for atmospheric modeling.

3.3 Theoretical calculations

The theoretical study of reaction (1) was performed using the DFT and Gn aforementioned methods. Results were compared to those of the reactions of OH with the propyne parent species, reaction (2), to help find an explanation of the differences in the reactivity of 2P1OL and its alkyne analogue. Experimental results reveal a significant increase in the rate coefficient from $(6.21 \pm 0.31) \times 10^{-12} \text{ cm}^3 \text{ molecule}^{-1} \text{ s}^{-1}$ in the reaction of P with OH [20], to $2.05 \times 10^{-11} \text{ cm}^3 \text{ molecule}^{-1} \text{ s}^{-1}$ in the reaction of 2P1OL with OH radicals as found in this work.



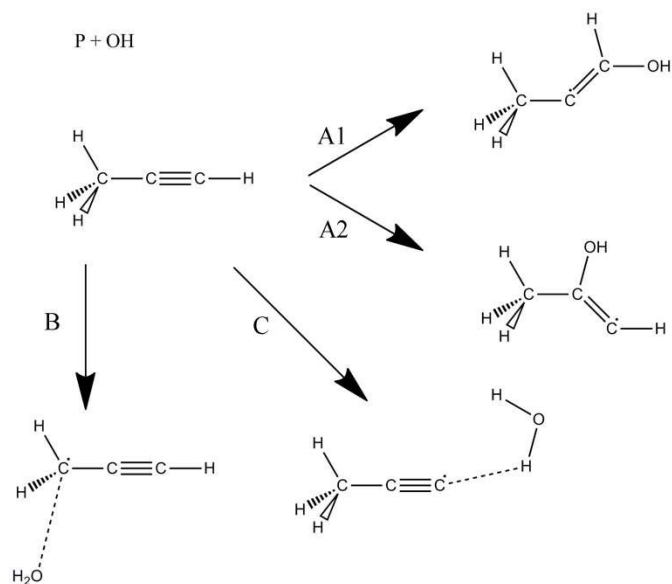
Scheme I. Addition (A1 and A2) and abstraction (B, C, D) reactions of 2P1OL with OH radicals.

This behavior could be explained by the possibility of formation of an intramolecular hydrogen bond which stabilizes the structure of the reaction intermediate [30] as observed in other similar compounds [31, 32]. However, the reason in the case of substituted alkynes was still unclear, since other explanations may exist. For that reason, we considered that it

was worthwhile to perform a deeper exploration from the molecular point of view. Several reaction paths were investigated for the reactions as summarized in Schemes I for 2P1OL and II for P. The first reaction studied was the addition of OH to the triple bond, which will be labeled reaction path A. Two additions are possible (to C2 or C3 in 2P1OL and to C1 or C2 in P. The other three reaction channels in the case of 2P1OL were the abstraction of hydrogen from the CH₂ (path B), OH (path D) and CH (path C) groups.

A previous study has shown that abstraction from a CH₃ group should be about 5 times more favorable than abstraction from an OH group (see, for instance, Xu and Lin on the reaction of OH with methanol and ethanol [33]). Channel C, corresponding to the abstraction of H from the CH group, was not thought to be important since the radical generated would be unstable. Transition states were identified in all cases and, in the case of paths A, B and D, the results for reactions of P and 2P1OL could be compared. The importance of reaction path C is negligible for P.

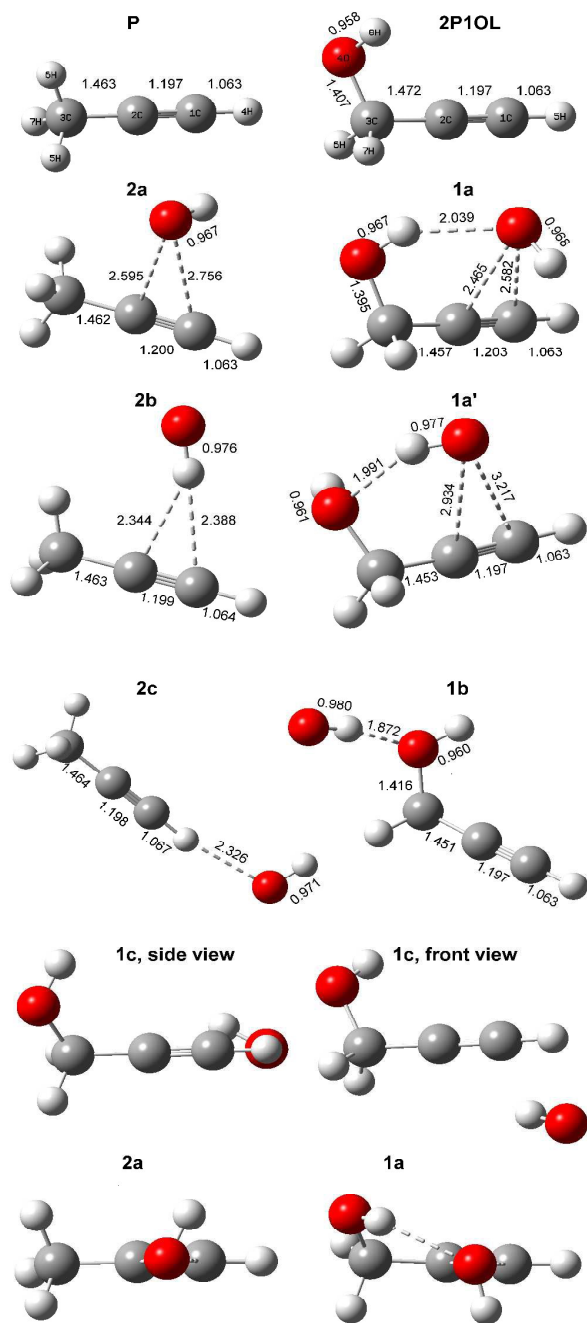
Reactants and Pre-barrier Complexes. The reactants and pre-barrier complexes obtained for reactions of 2P1OL and P with OH radicals are shown in Figure 2.



Scheme II. Addition (A1 and A2) and abstraction (B, D) reactions of P with OH radicals.

Several pre-barrier complexes were identified. In the case of 2P1OL, 1a corresponds to the complex leading to either addition to the triple bond, or removal of the OH hydrogen. 1b corresponds to the initial complex leading to hydrogen abstraction from the CH₂ group, and 1c corresponds to the initial complex leading to abstraction of the CH hydrogen. Two views of the latter are shown in Figure 2 to appreciate the relative arrangement of the OH reactant with respect to the

C—H bond. Additionally, a less stable isomer of the pre-



reactive complex 1a, identified as 1a', was found.

Figure 2. Structure of propyne (P), propargyl alcohol (2P1OL) and the initial complexes for reactions (1) and (2) at the BMK/6-311++G(2df,2pd) level. Species 2a, 2b and 2c are the IC for P; species 1a, 1a', 1b and 1c the IC for 2P1OL. Last two drawings show a comparison between the 1a (2P1OL) and 2a.

In this case the hydrogen bond is established between the hydrogen of the incoming hydroxyl radical and the oxygen of the alcohol group. In the case of P, 2a is the initial complex

leading to addition. The comparison of front views of both 1a and 2a initial complexes show large similarities; the oxygen atom of the incoming OH is located midway between the carbon atoms but the C₁—O and C₂—O distances are both about 0.04 Å shorter for 2P1OL than for P. This is an effect of the hydrogen bond stabilization produced by the hydroxyl substituent in 2P1OL (the H⁺OH distance is 2.090 Å and the O—H⁺O angle is 142 deg at the BMK/6-311++G(2df,2pd) level of theory).

In the case of P, two other initial complexes, leading to hydrogen abstraction, were also identified. 2b is similar to 2a in the triangular disposition, but it is the hydrogen of the OH the one directed toward the carbons (in a similar disposition to the initial complex for the addition of hydrogen halides to alkenes in gas phase). This conformation allows the oxygen atom to be at a favorable geometry for abstraction of a hydrogen atom from the CH₃ group. The third pre-reactive complex found for P shows a structure where the oxygen of the OH is clearly linked to the hydrogen of the CH group. The structure is more clearly pointing to the abstraction than in the case of 1c, but intrinsic reaction paths (IRC) calculations show that both are the correct initial complexes for those abstraction channels in their respective potential energy surfaces.

Transition states. All reactions channels shown in Schemes I and II were investigated independently. Transition states were found in all cases, implying that none of the reactions is barrierless. Kinetic considerations can then, in principle, be derived from the height of the barriers and will be discussed later. The structures of all transition states found are shown in Figure 3. Some important geometrical parameters are reported at the BMK/6-311++G(2df,2pd) level only, since no essential variations were found when using different theoretical methods for the geometry optimization.

Two transition states TS1A1 and TS1A2 were found for the addition of OH to 2P1OL, as well as for the addition to P, TS2A1 and TS2A2. The effect of the hydroxyl group in propargyl alcohol is clearly seen from the comparison of the structures. For the addition at C3 in 2P1OL (C1 in P), the hydroxyl in propargyl alcohol “hooks” the incoming hydroxyl radical, the CCO angle is then reduced about 10 deg, the O—C₁ distance is slightly increased, and a hydrogen bond is formed. The hydrogen of the incoming hydroxyl group is then pointing away from the triple bond, while in the addition to P is pointing towards the triple bond. In the case of the addition to C2 it is possible to observe a different effect. The hydroxyl of 2P1OL is not hydrogen bonded to the incoming hydroxyl. All efforts to locate a structure with such a bonding pattern were failing. Furthermore, the angle between the triple bond and the forming C—O bond is more closed in 2P1OL than in the addition to P.

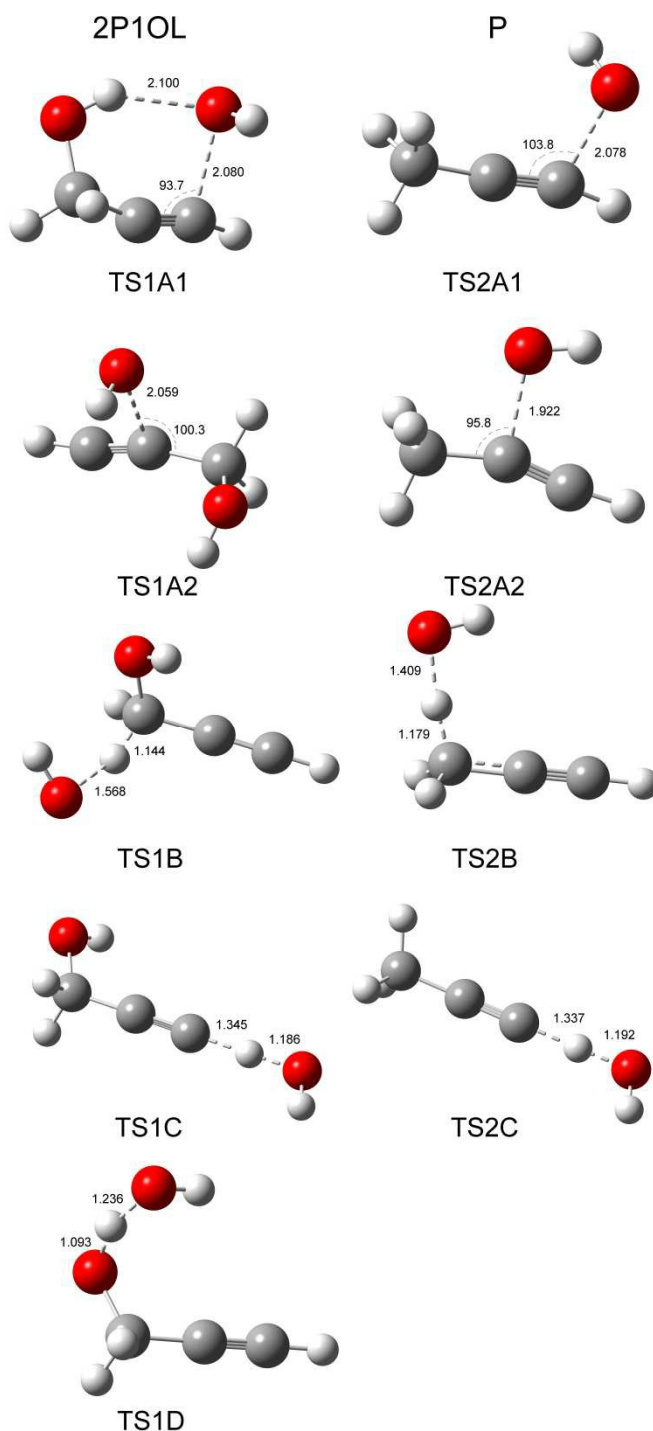


Figure 3. Transition states corresponding to 2P1OL (TS1) and P (TS2) at the BMK/6-311++G(2df,2pd) level. Transition states A1 and A2 correspond to the addition reactions on C1 and C2 respectively. Transition states B, C and D correspond to hydrogen abstraction from CH₂, CH and OH respectively. Important geometrical parameters are displayed (in Å).

Consequently, it may be concluded that the effect of the OH in 2P1OL with respect to the addition in C2 is relatively weak and thus the addition at C2 would be similar in 2P1OL and P.

In the case of the hydrogen abstraction reactions, there are also some noticeable differences between the transition states of 2P1OL and P. In the case of abstraction from CH₂OH in 2P1OL and from CH₃ in P, TS1B and TS2B, the transition state appears earlier for the former than for the latter (the C—H distance in the former is about 0.04 Å shorter while the forming OH bond is larger in TS1B than in TS2B). This is clearly an effect of the hydroxyl group present in 2P1OL, since no such difference between the transition states is observed for TS1C and TS2C (corresponding to the abstraction of hydrogen from the CH group).

It is also noticeable that the HOCO dihedral angle is close to zero, another indication of the directing influence the OH of 2P1OL is having in the reaction. On the other side, the abstraction of the H bond from the CH group is similar in both 2P1OL and P. The only difference is that the transition state occurs later in 2P1OL than in P (the CH distance is larger and the OH distance shorter in TS1C than in TS2C). Finally, it is clear that abstraction of the hydrogen atom from the 2P1OL hydroxyl group occurs through a transition state that has no involvement of the triple bond. The height of the barriers and the reaction paths will be discussed later.

Products. The structure of the products obtained for the reactions paths A-D depicted in Schemes I and II are shown in Figures 4 and 5. Within the atmosphere, once the addition or abstraction have occurred, the radical will further react with oxygen according to a reasonably well established path [34] which lead to a mixture of aldehydes, ketones and acids. In the absence of oxygen, however, the radicals have other reaction

channels available. Condensation, internal rearrangement or reaction with the water molecule produced in the abstraction, are possible reaction paths. Despite its lack of interest in the context of atmospheric chemistry, we explored the channels of hydrogen atom internal transfer and reaction with the water

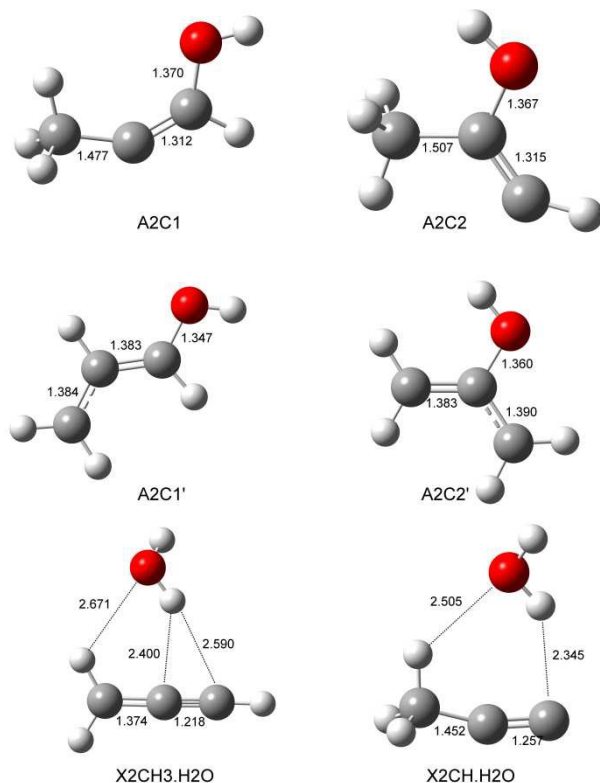
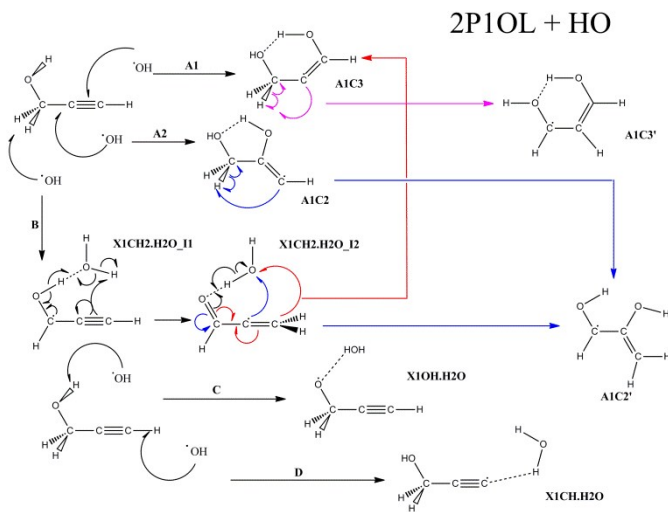


Figure 4. Structure of the products and intermediates obtained for the reaction of propyne with OH at the BMK/6-311++G(2df,2pd) level. Some of the important interatomic distances are shown (in Å)



Scheme III. Complete scheme of addition, abstraction, internal rearrangement and reaction with water of the radicals formed in the reaction of 2P1OL with OH.

molecule, to obtain a more comprehensive picture of the potential energy surface for the reaction of 2P1OL with OH. The resulting interconnected products are shown in Scheme III and the structures of these products have also been included in Figures 4. We will later discuss the thermochemical and kinetic implications of these channels.

In the case of 2P1OL, the addition radical A1C3 is the one that leads to the observed products of oxidation, if oxygen is present in the reaction mixture. A hydrogen migration may occur from C1 to C2, leading to the very stable A1C3' radical (see later for the thermochemical results). Similarly, the A1C2 product of the addition of OH to the C2 carbon in 2P1OL may lead by an H-atom internal migration from C1 to C3 to the planar stable radical A1C2'.

As shown in Scheme III, the abstraction intermediate X1CH₂.H₂O_{I1} may isomerize to X1CH₂.H₂O_{I2}, a structure which may further undergo a reaction between the radical and water. This may lead in turn, through different paths, to the products A1C3 or A1C2'. The complexes X1OH.H₂O and

X1CH.H2O do not participate in these reactions and may easily decompose, releasing water, and/or react with another radical present in the media. These reactions have not been investigated further.

As can be seen from the comparison of the structures in Figures 4 and 5, the presence of the hydroxyl group in 2P1OL essentially determines the conformation of the stable isomers, due to the presence of the hydrogen bond. In the case of propyne, there are no structures analogue to X1CH2.H2O_I2 or

Table 2. Energetics of the pre-reactive complexes with respect to the separated reactants (in kcal/mol)

Complex	Method	ΔE	$\Delta(E+ZPE)$	ΔH_{298}°	ΔG_{298}°
1a	M06	-8.8	-6.7	-7.3	1.3
	BMK	-5.7	-4.2	-4.6	3.4
	G2	-4.1	-4.4	-4.7	2.7
	G4	-2.8	-2.8	-3.4	5.2
1a'	M06	-6.2	-4.3	-4.8	2.5
	BMK	-5.2	-3.3	-3.7	3.1
	G2	-4.0	-4.3	-4.6	1.7
1b	G4	-4.8	-4.9	-5.4	2.1
	M06	-6.2	-4.2	-4.8	3.0
	BMK	-5.3	-3.6	-3.9	2.5
1c	G2	-4.0	-4.3	-4.6	1.7
	G4	-4.8	-4.9	-5.4	2.1
	M06	-6.2	-4.4	-4.8	2.5
	BMK	-5.2	-3.3	-3.7	3.1
2a	G2	-4.0	-4.3	-4.6	1.7
	G4	-4.8	-4.9	-5.4	2.1
	M06	-5.3	-4.0	-4.2	2.3
2b	BMK	-2.8	-1.5	-1.6	4.6
	G2	-2.3	-2.7	-2.9	3.3
	G4	-0.5	-0.9	-1.1	5.6
2c	M06	-4.4	-3.2	-3.4	3.1
	BMK	-3.5	-2.1	-2.3	4.2
	G2	-2.3	-2.7	-2.9	3.3
2c	G4	-2.8	-3.1	-3.4	3.6
	M06	-1.4	-0.7	-1.0	5.5
	BMK	-0.9	-0.1	0.2	5.3
2c	G2	-2.3	-2.7	-2.9	3.3
	G4	-1.2	-1.5	-1.8	4.7

X1OH.H2O, but there also exist the more stable planar isomers A2C1' and A2C2'. This latter structure is particularly interesting and worth a deeper examination than that done in this work.

Thermochemistry. It is generally accepted that the reaction of oxygen atoms and OH radicals with unsaturated hydrocarbons proceeds through addition mechanisms [35, 36] and exhibits negative temperature dependence, a characteristic of barrierless reactions [37, 38]. However, this can also be explained simply by the formation of a pre-reactive complex without barrier and a further reaction of this complex toward the radical product across a small energy barrier [39]. In a previous study of the reaction of OH radicals with 2P1OL [14], the authors performed approximate calculations on the stability of the radicals formed after addition of OH to C2 and C3 of 2P1OL. They concluded that the product of the former attack was the more stable, although they did not calculate the

structure and energetics of any possible pre reactive complexes.

Relative energies of the pre-reactive complexes with respect to the isolated OH and P or 2P1OL reactants are shown in Table 2. Several features can be observed from the data listed. In the first place, it is clear that neither of these complexes is stable at room temperature (since for all of them $\Delta G_{298}^\circ > 0$). Although formation of all the complexes is exergonic, the entropic term more than for compensates the enthalpy, and the free energy of formation is thus always positive. Therefore, only at low temperature these pre-reactive complexes might be observed spectroscopically.

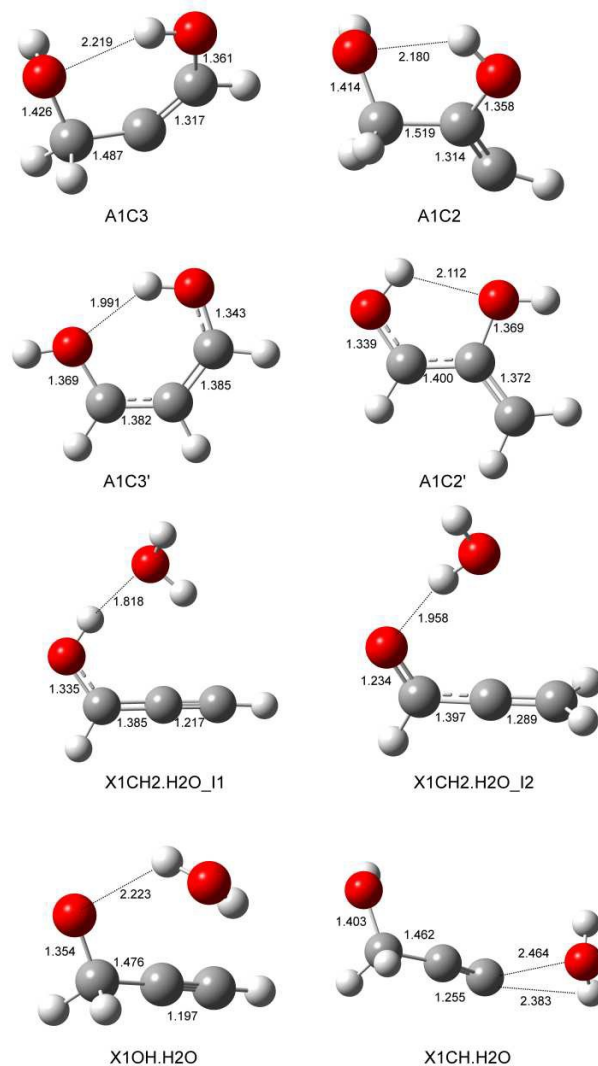


Figure 5. Structure of the products and intermediates obtained for the reaction of 2P1OL with OH at the BMK/6-311++G(2df,2pd) level. Some of the important interatomic distances are shown (in Å)

In the second place, looking to the precision of the calculations, it can be seen that different methods give results which are very close. The best results obtained for ΔG°_{298} , at the BMK/6-311++G(2df,2pd) and G4 levels, do not differ in more than 2 kcal/mol both for P and 2P1OL. The fact that methods based on very different levels of calculation give similar results lends credibility to the quantitative conclusions that may be reached.

In the third place, considering now only the two complexes of propyne, 2a and 2b, we conclude that their relative stability is

dependent on the accuracy of the methods. Less accurate methods predict both pre-reactive complexes to be of similar stability at very low temperatures, while the more accurate methods (BMK and G4) predict 2b to be the most stable. As we pointed out before, this fact is negligible at room temperature, since entropy overrules enthalpy and the pre-reactive complexes would not be stable. Finally, considering now the three pre-reactive complexes of 2P1OL, it can be seen that they have almost all the same stabilization energy.

Table 3. Relative energies of reaction for the five different reactions pathways (1) and (2). Energies in kcal/mol. Enthalpies and free energies calculated at 298K. Last column shows the difference in reaction enthalpies with respect to the most stable products A1C3' for 2P1OL and A2C2' for P.

Reaction	Method	ΔE	$\Delta(E+ZPE)$	ΔH_{298K}°	ΔG_{298K}°	$\Delta\Delta H_{298K}^{\circ}$
2P1OL+ HO \rightarrow A1C3	M06/6-311++G(2df,2pd)	-42.3	-37.0	-38.5	-28.1	32.0
	BMK/6-311++G(2df,2pd)	-40.4	-35.0	-36.5	-26.1	34.7
	G2	-33.2	-32.4	-33.8	-23.7	33.0
	G4	-33.5	-32.6	-34.1	-23.7	32.9
2P1OL+ HO \rightarrow A1C3'	M06/6-311++G(2df,2pd)	-73.7	-69.0	-70.5	-60.0	0.0
	BMK/6-311++G(2df,2pd)	-74.6	-66.2	-71.2	-61.0	0.0
	G2	-66.2	-65.2	-66.8	-56.0	0.0
	G4	-66.4	-65.2	-67.0	-55.8	0.0
2P1OL+ HO \rightarrow A1C2	M06/6-311++G(2df,2pd)	-40.0	-35.5	-37.0	-26.5	33.5
	BMK/6-311++G(2df,2pd)	-38.9	-34.3	-35.8	-25.2	35.5
	G2	-33.1	-32.4	-33.7	-23.5	33.0
	G4	-33.4	-32.5	-34.0	-23.4	33.0
2P1OL+ HO \rightarrow A1C2'	M06/6-311++G(2df,2pd)	-73.1	-69.1	-70.6	-60.0	-0.1
	BMK/6-311++G(2df,2pd)	-73.7	-69.5	-71.0	-60.3	0.2
	G2	-65.7	-65.2	-66.3	-56.6	0.5
	G4	-65.6	-64.9	-66.2	-55.9	0.8
2P1OL+ HO \rightarrow X1CH2 + H2O	M06/6-311++G(2df,2pd)	-38.4	-38.6	-38.4	-39.2	32.1
	BMK/6-311++G(2df,2pd)	-35.5	-36.0	-35.7	-36.7	35.5
	G2	-34.2	-34.8	-34.2	-35.7	32.6
	G4	-35.6	-35.7	-35.6	-36.3	31.4
2P1OL+ HO \rightarrow X1CH + H2O	M06/6-311++G(2df,2pd)	11.6	12.8	12.9	12.0	83.4
	BMK/6-311++G(2df,2pd)	15.7	15.0	15.3	14.1	86.5
	G2	20.3	20.0	20.3	19.1	87.1
	G4	14.2	14.0	14.2	12.1	81.2
2P1OL+ HO \rightarrow X1COH + H2O	M06/6-311++G(2df,2pd)	-13.3	-14.6	-14.4	-15.2	56.1
	BMK/6-311++G(2df,2pd)	-12.9	-13.8	-13.8	-14.5	57.5
	G2	-11.5	-11.6	-11.5	-12.2	55.3
	G4	-12.6	-12.7	-12.6	-13.4	54.4
P + HO \rightarrow A2C1	M06/6-311++G(2df,2pd)	-37.2	-32.8	-33.9	-24.8	24.2
	BMK/6-311++G(2df,2pd)	-36.2	-31.3	-32.6	-23.1	25.8
	G2	-29.1	-28.7	-29.7	-20.9	26.1
	G4	-29.4	-28.8	-30.0	-20.8	25.5
P + HO \rightarrow A2C1'	M06/6-311++G(2df,2pd)	-60.3	-56.0	-57.5	-47.3	0.7
	BMK/6-311++G(2df,2pd)	-61.6	-56.9	-58.5	-48.1	0.0
	G2	-54.2	-53.5	-54.8	-45.0	1.0
	G4	-53.8	-52.8	-54.4	-44.0	1.1
P + HO \rightarrow A2C2	M06/6-311++G(2df,2pd)	-35.0	-31.0	-32.3	-22.6	25.9
	BMK/6-311++G(2df,2pd)	-33.9	-29.9	-31.1	-21.7	27.4
	G2	-28.6	-28.2	-29.2	-21.2	26.7
	G4	-28.8	-28.1	-29.4	-19.7	26.1
P + HO \rightarrow A2C2'	M06/6-311++G(2df,2pd)	-60.4	-56.6	-58.2	-47.9	0.0
	BMK/6-311++G(2df,2pd)	-61.0	-56.8	-58.4	-48.0	0.0
	G2	-55.2	-54.5	-55.8	-45.9	0.0
	G4	-54.9	-53.8	-55.5	-45.0	0.0
P + HO \rightarrow X2CH3 + H2O	M06/6-311++G(2df,2pd)	-28.7	-29.7	-29.3	-30.3	28.8
	BMK/6-311++G(2df,2pd)	-26.0	-27.0	-26.6	-27.6	31.8
	G2	-26.4	-26.9	-26.4	-27.7	29.4
	G4	-27.0	-27.4	-27.0	-28.0	28.5
P + HO \rightarrow X2CH + H2O	M06/6-311++G(2df,2pd)	11.8	13.0	13.2	12.2	71.4
	BMK/6-311++G(2df,2pd)	16.4	15.5	15.8	14.6	74.3
	G2	14.3	13.9	14.3	12.5	70.2
	G4	14.5	14.2	14.5	13.1	70.0

The only case in which there is an important difference between results of different methods is for the 1a complex in which the G4 results are way off the other methods. In all cases, the pre-reactive complexes of 2P1OL are more stable

than those with P, due to the influence of the OH group. A second aspect concerning the thermodynamics of these reactions is to consider the heats and the reaction free energies.

The relative energies of the different intermediates and products have been collected in Table 3 for both P and 2P1OL. In the last column of this table we show the relative enthalpies at 298.15K with respect to the most stable product. Both for the parent alkyne and for 2P1OL, the rearranged planar radicals are by far the most stable products. Whether these products could be obtained will depend on the height of the barriers, which we will discuss later. From the thermochemical point of view though, A1C3' and A1C2' for 2P1OL, and A2C1' and A2C2' for P, would be the preferred products of the reactions (1) and (2). On the other hand, as would be expected, the abstraction reaction from the terminal carbon is the one that gives the least stable product by far, both for P and 2P1OL. The presence of the hydroxyl group in 2P1OL does not affect at all the outcome of this reaction.

From thermochemistry, the additions to C3 in 2P1OL or to C1 in P are slightly more favorable than the additions to C2 (between 1 and 2 kcal/mol). In both cases the abstraction reaction at C1 in 2P1OL or C3 in P is more favorable than either addition. The main difference between the reactions of P and 2P1OL is that abstraction is thermochemically about two times more favorable than addition in the latter species. This is of course due to the presence of the OH in X1CH2.H2O_I1 and its absence in X2CH3.H2O, the hydrogen bond providing for the extra energy of the former product.

Considering the different methods of calculation, relatively large discrepancies can be seen in the results (up to 5 kcal/mol). However, due to the large value of the enthalpies of reaction, the discrepancies are not larger than 10% of the respective values. This would be then the expected accuracy of our thermochemical calculations, although probably it is an upper limit and the results with the best methods are more accurate.

Reaction paths and kinetics. The general scheme of relative energies of intermediate, products and transition states for the reaction of 2P1OL with OH is shown in Figure 6. Values shown include the zero-point energy for each species. The relative energy of the transition states with respect to the reactants, as well as the barriers for the different reactions are collected in Table 4.

As shown above, all the pre-reactive complexes are more stable than the separated reactants at 0 K. Compared to the relative energies of other intermediates and products, the separation between the stability of the different pre-reactive complexes are quite minor. The transition states for the addition to C1, TS1A1, and the abstraction of hydrogen from C1, TS1B, are both below the energy of the separated reactants (about -2 and -1 kcal/mol respectively), thus confirming the experimentally observed negative Arrhenius behavior. The transition states for the addition to C2 and the abstraction of the hydrogen from the hydroxyl group, TS1A2 and TS1C respectively, are instead above the energy of the separated reactants (by about 1 and 2 kcal/mol respectively).

The transition state for the abstraction of hydrogen from C3 is energetically unfavorable (about 30 kcal/mol) and therefore considered negligible in the present analysis.

As pointed out before, the hydrogen abstraction product from C1, X1CH2.H2O_I1, is lower in energy than the addition product, A1C3, which is in turn lower than the product of hydrogen abstraction from the hydroxyl group, X1OH.H2O. The fate of the addition and abstraction products is quite different. A1C3 can suffer an internal rearrangement through a 1,2 hydrogen migration and end up giving the A1C3' final product. The corresponding transition state, TS1I, is however quite high, its energy being above that of the separated products (between 3 and 7 kcal/mol, depending on the method of

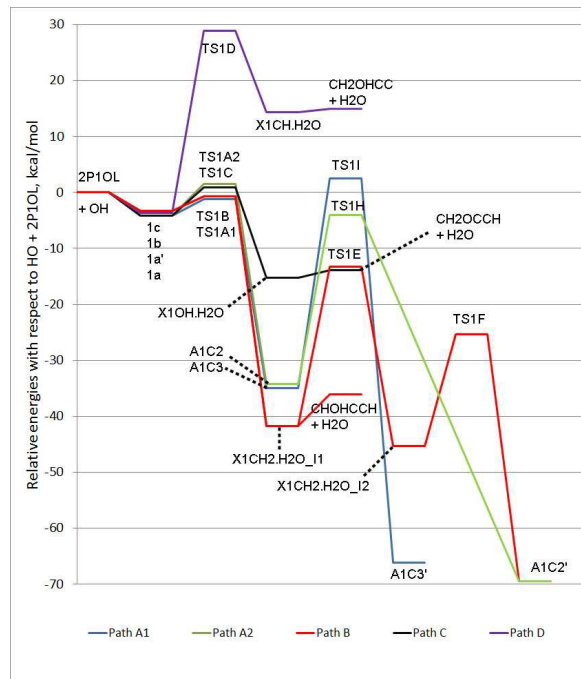


Figure 6. Relative E+ZPE energies for products, intermediates and transition states for the reaction of 2P1OL with OH radicals (in kcal/mol) with respect to the reactants. The values shown were calculated at the BMK/6-311++G(2df,2pd) level.

calculation) and the barrier is substantial (about 38-40 kcal/mol). This fact seems to suggest that the A1C3 → A1C3' reaction would not occur. However, since this is a proton migration between two neighboring atoms, quantum tunneling is very likely to happen.

Table 4. Relative E+ZPE energies for products, intermediates and transition states for the reaction of 2P1OL with HO (in kcal/mol) with respect to the reactants.

Transition State	Method	Relative energy			Barrier		
		$\Delta(E+ZPE)$	ΔH_{298K}°	ΔG_{298K}°	$\Delta(E+ZPE)$	ΔH_{298K}°	ΔG_{298K}°
TS1A1	M06	-4.7	-5.9	3.8	1.9	1.4	3.8
	BMK	-1.1	-2.3	7.4	3.0	2.3	7.4
	G2	-1.1	-1.9	6.9	3.3	2.8	6.9
	G4	-1.0	-2.2	7.6	1.8	1.3	7.6
TS1A2	M06	-1.5	-2.4	6.8	1.9	1.4	6.8
	BMK	1.5	0.7	9.5	5.7	5.3	9.5
	G2	1.1	0.3	9.3	5.5	5.0	9.3
	G4	0.9	0.0	9.2	3.7	3.4	9.2
TS1B	M06	-3.1	-3.9	4.6	1.0	0.8	4.6
	BMK	-0.7	-1.4	6.7	2.9	2.6	6.7
	G2	-0.7	-0.7	4.3	3.6	3.8	4.3
	G4	-0.4	-1.2	7.6	4.5	4.1	7.6
TS1C	M06	-1.8	-2.8	6.3	2.5	2.0	6.3
	BMK	0.9	0.1	8.7	4.2	3.8	5.6
	G2	3.8	2.9	11.8	8.1	7.5	11.8
	G4	3.4	2.6	11.3	8.3	7.9	11.3
TS1D	M06	23.0	22.5	30.4	27.3	27.2	30.4
	BMK	28.9	28.2	36.4	32.2	32.0	36.4
	G2	25.2	25.1	31.3	29.5	29.6	31.3
	G4	36.1	35.6	43.3	41.0	40.9	43.3
TS1E	M06	-17.5	-19.2	-8.3	27.9	26.6	29.6
	BMK	-13.3	-14.9	-4.1	28.4	26.9	30.3
	G2						
	G4	-11.7	-13.4	-2.4	29.3	27.9	30.9
TS1F	M06	-27.8	-29.5	-18.5	19.1	17.5	21.8
	BMK	-25.4	-27.1	-16.1	19.9	18.1	23.2
	G2	-21.9	-23.2	-13.0			
	G4	-21.6	-23.4	-12.3	20.3	18.5	23.5
TS1G	M06	-12.5	-14.4	-3.0	34.4	32.6	37.2
	BMK	-9.1	-11.0	0.3	36.2	34.2	39.5
	G2	-4.7	-6.6	4.5			
	G4	-5.4	-7.3	4.1	36.6	34.7	39.8
TS1H	M06	-3.0	-4.6	6.2	32.5	32.4	32.6
	BMK	-4.0	-5.6	5.1	30.2	30.1	30.3
	G2	0.4	-1.0	9.4	32.8	32.8	32.8
	G4	0.1	-1.5	9.2	32.5	32.5	32.6
TS1I	M06	-0.6	-2.1	8.5	35.9	35.8	36.2
	BMK	2.5	0.8	11.6	37.5	37.3	37.7
	G2	0.1	-1.3	9.1	32.6	32.5	32.8
	G4	7.3	5.8	16.3	39.9	39.9	40.0
TS2A1	M06	-2.9	-3.6	4.3	1.2	0.6	4.3
	BMK	0.1	-0.6	7.0	1.6	1.1	7.0
	G2	0.7	0.0	8.1	3.9	3.5	8.1
	G4	0.1	-0.6	7.1	0.9	0.4	7.1
TS2A2	M06	-2.5	-3.3	5.2	1.5	0.8	5.2
	BMK	0.8	-0.1	8.4	2.3	1.6	8.4
	G2	0.7	0.0	8.1	3.4	2.9	8.1
	G4	0.8	-0.1	8.5	1.6	1.0	8.5
TS2B	M06	-1.8	-2.6	5.5	1.4	0.8	5.5
	BMK	0.9	0.1	8.1	3.0	2.4	8.1
	G2	1.6	1.0	8.8	4.4	3.9	8.8
	G4	2.2	1.7	8.7	5.3	5.1	8.7
TS2C	M06	23.6	22.6	31.2	24.3	23.6	31.2
	BMK	29.2	28.6	36.4	29.3	28.5	36.4
	G2	17.1	17.0	23.0	19.8	19.9	23.0
	G4	18.3	17.8	24.6	19.8	19.5	24.6

This point has not been explored further in this work, but it is worth to keep it in mind for future work. At any rate, the presence of O₂ in the atmosphere would allow alternative reactions to take place and products from A1C3' may well be never observed.

On the other side, the X1CH2.H2O_I1 intermediate can release water, since the complex is not exceedingly stable with respect to the separated species, or can rearrange to give the X1CH2.H2O_I2 complex. The energy of the corresponding transition state, TS1E, is much lower than the sum of the

energies of 2P1OL and OH (about -12 kcal/mol) and the isomer I2 is more stable than I1. Thus, both from the thermodynamic and kinetic points of view, this is a feasible reaction. In turn, X1CH2.H2O_I2 can proceed further to A1C2' since the transition state TS1F is even lower than TS1E (about -22 kcal/mol), the barrier is smaller than for the reverse reaction (about 20 kcal/mol) and A1C2' is more stable than either X1CH2.H2O_I1 or X1CH2.H2O_I2. Although it is clear that these reactions would not proceed in the atmosphere (since the presence of O₂ would lead to the opening of other reaction channels) further research is necessary to know whether this reaction path is competitive with the possible condensation reactions starting from X1CH2.H2O_I1.

As was shown in Scheme III, an alternative path exists starting from X1CH2.H2O_I2, leading to A1C3. This path was not depicted in Figure 6 to avoid excessive complexity.

The corresponding transition state is TS1G and although it is more stable than the isolated reactants (between 5 and 9 kcal/mol) the barrier is larger (about 40 kcal/mol as compared to the 20 kcal/mol necessary to rearrange to A1C2').

The general picture emerging from these considerations is that abstraction of hydrogen from the C1 atom in 2P1OL is at least as favorable as addition to the C3 carbon. The free energy of activation for the addition and abstraction reactions are 7.4 and 6.7 kcal/mol at the BMK/6-311++G(2df,2pd) level and 7.6 and 7.6 kcal/mol at the G4 level respectively. In the absence of oxygen then, and leaving aside the possible condensation reactions, our calculations suggest that the A1C3 and A1C2' radicals would be the resulting species of the reactions.

The global comparison of these results with those of propyne shows an interesting difference. The addition and abstraction reactions in the case of P have free energies of activation of about 7 and 9 kcal/mol. While the addition reaction is predicted theoretically to be as fast in 2P1OL as it is in P, within the precision of the methods of calculation, the abstraction reaction is about one order of magnitude faster in 2P1OL than in P, providing then support to the experimental three times larger speed of the reaction of OH with 2P1OL than with P.

It must be stated that theoretical methods are not able to describe precisely such a small difference between the rate constants as found in this study. Since the free energy of activation participates in the exponent for the evaluation of rate constants, a difference in accuracy of 1 kcal/mol (smaller than that obtainable with practically all theoretical methods) shields a factor of five in the value of the rate constant. Thus, the computational studies, although can be useful for understanding qualitatively and semi-quantitatively the reaction paths of a given reaction system, are not able to produce rate constants with an accuracy similar to the experimental measurements.

4. Conclusions

The rate coefficient for the reaction of propargyl alcohol with OH radicals has been determined using gas chromatography with flame ionization detection (GC/FID) at 298 K and atmospheric pressure. The experimental value obtained by the relative method using methyl methacrylate and butyl acrylate as references was $(2.05 \pm 0.30) \times 10^{-11} \text{ cm}^3 \text{ molecule}^{-1} \text{ s}^{-1}$. The rate coefficient obtained in this work at atmospheric pressure is more than double the value reported in a previous determination between 1.33-2.67 kPa in He, where probably the high pressure limit of *k* was not achieved. Consequently, the present determination constitutes the first determination at atmospheric pressure and could be considered as a recommended value for use in atmospheric modeling.

To explain the differences in reactivity of 2P1OL and its analogue alkyne (P), DFT and *ab initio* composite models calculations on the reactants, intermediates, transition states and products were performed. From both the thermodynamic and kinetic points of view, it was determined that addition of OH to the end carbon at the triple bond (C1 in P, C3 in 2P1OL) occurs preferentially with respect to the addition to the middle C2 carbon. As found in other studies, addition is preferred over abstraction for the alkyne, but it was determined in this study that abstraction should proceed faster than addition in 2P1OL. The results suggest that addition proceed to give a product similar to that obtained for propyne, only that it is thermodynamically more stable because of the hydrogen bonding produced by the hydroxyl group in propargyl alcohol. The abstraction reaction, on the other side, should proceed through a pair of intermediate species, where water forms a complex with different isomers of the radical formed, to give the very stable A1C2' radical. Abstraction is about 7 to 11 times faster in 2P1OL than in P and, together with the fact that addition proceeds at more or less the same rate, should explain why the experimental rate constant for the reaction of 2P1OL with OH is about three times larger than that for the reaction of propyne with OH.

Acknowledgements

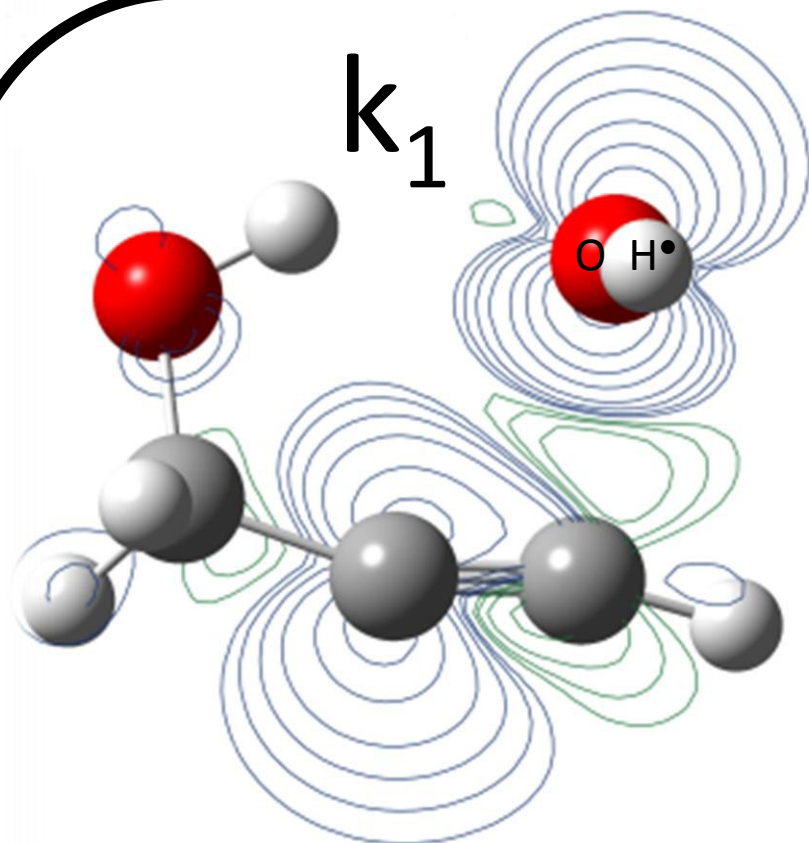
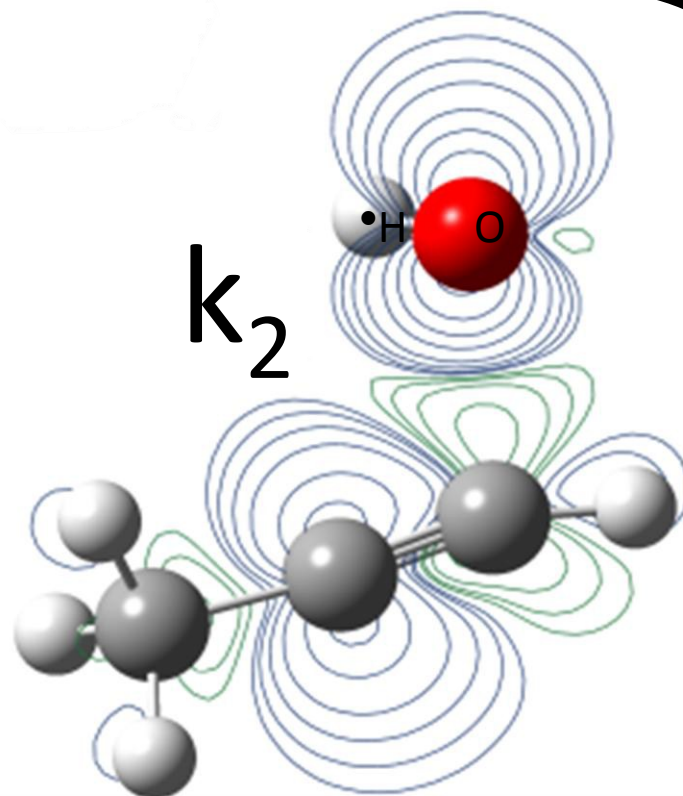
The authors wish to acknowledge SECYT (Argentina), CONICET (Argentina), ANPCyT (Préstamo BID 1201/OC-AR), Agencia Córdoba Ciencia, SECyT-UNC (Córdoba, Argentina), PEDECIBA (Uruguay), CSIC-UdelaR (Uruguay) and ANII (Uruguay) for financial support of this research. R. G. G. wish to thank CONICET for a PhD fellowship.

Notes and references

^a INFIQC (CONICET- Facultad de Ciencias Químicas, Universidad Nacional de Córdoba).Dpto. de Físicoquímica, Ciudad Universitaria, 5000 Córdoba, Argentina.

^b CCBG, DETEMA, Facultad de Química, Universidad de la República, CC1157, 11400 Montevideo, Uruguay.

- 1 B. J. Finlayson-Pitts and J. N. Pitts, Jr., *Chemistry of the Upper and Lower Atmosphere: Theory, Experiments, and Applications*. Academic Press, New York, 1999.
- 2 J. Lockhart, M. A. Blitz, D. E. Heard, P. W. Seakins, R. J. Shannon, J. Phys. Chem. A, 2013, **11**, 75407–5418.
- 3 Y. Feng, K. S. Siow, W. K. Teo, A. K. Hsieh, Corrosion Sci., 1999, **41**, 829–1030, and references therein.
- 4 E. Duwell, J. Electrochem. Soc., 1962, **109**, 1013–1017.
- 5 B. B. Pati, P. Chatterjee, T. B. Singh, D. D. N. Singh, Corrosion, 1990, **46**, 354–359
- 6 R. Atkinson, J. Phys. Chem. Ref Data, Monograph 1, 1989.
- 7 S. Hatakeyama, N. Washida, H. Akimoto, J. Phys. Chem., 1986, **90**, 173–178.
- 8 B. Bohn, Siese, M. Zetzsch, C., J Chem. Soc. Faraday Trans., 1996, **92**, 1459–1466.
- 9 R. Atkinson, J. Arey, Chem. Rev., 2003, **103**, 4605–4638.
- 10 Y. Gai, M. Ge, W. Wang, Atm. Env., 2011, **45**, 53–59.
- 11 F. Bernard, V. Daële, A. Mellouki, J. Phys. Chem. A, 2012, **116**, 6113–6126.
- 12 T. Imamura, Y. Iida, K. Obi, I. Nagatani, K. Nakagawa, I. Patroescu-Klotz, S. Hatakeyama, Published online in Wiley InterScience (www.interscience.wiley.com).
- 13 J. R. Wells, Int. J. Chem. Kinet., 2004, **36**, 534–544.
- 14 H. P. Upadhyaya, A. Kumar, P. D. Naik, A. V. Sapre, J. P. Mittal, Chem. Phys. Lett., 2001, **349**, 279–285.
- 15 A. Maranzana, G. Ghigo, G. Tonachini, J. R. Barker, J. Phys. Chem. A., 2008, **112**, 3656–3665.
- 16 J. Calvert, A. Mellouki, J. Orlando, M. Pilling, T. Wallington. Mechanisms of Atmospheric Oxidation of the Oxygenates. Oxford University Press, 2011.
- 17 C. Papagni, J. Arey, R. Atkinson, Int. J. Chem. Kinet., 2001, **33**, 142–147.
- 18 J. J. Orlando, G. S. Tyndall, N. Ceazan. J. Phys. Chem. A, 2001, **105**, 3564–3569.
- 19 A. Le Person, G. Solignac, F. Oussar, V. Daële, A. Mellouki, R. Winterhalter, G.K. Moortgat. Phys. Chem. Chem. Phys., 2009, **35**, 7619–7628.
- 20 R. Atkinson, S. M. Aschmann. Int. J. Chem. Kin., 1984, **16**, 259–268.
- 21 Y. Zhao, D. G. Truhlar. Theor. Chem. Acc., 2008, **120**, 215–241.
- 22 A. D. Boese, J. M. L. Martin. J. Chem. Phys., 2004, **121**, 3405–3416.
- 23 S. Peirone, J. D. Nieto, P. M, Cometto, T. d. S. Barbosa, G.F. Bauerfeldt, G.Arbilla, S. I. Lane, J. Phys. Chem. A, 2015, **119**, 3171–3180.
- 24 A. K. Wilson, K. A. Peterson, S. E. Woon, Theor. Chem. Acc., 2015, **134**, 1–4
- 25 L. A. Curtiss, K. Raghavachari, G. W. Trucks, J. A. Pople. J. Chem. Phys., 1991, **94**, 7221–7230.
- 26 L. A. Curtiss, P. C. Redfern, K. Raghavachari. J. Chem. Phys., 2007, **126**, 84–108.
- 27 Gaussian 09, Revision D.01, Frisch, M. J.; Trucks, G. W.; Schlegel, H. B.; Scuseria, G. E.; Robb, M. A.; Cheeseman, J. R.; Scalmani, G.; Barone, V.; Mennucci, B.; Petersson, G. A.; Nakatsuji, H.; Caricato, M.; Li, X.; Hratchian, H. P.; Izmaylov, A. F.; Bloino, J.; Zheng, G.; Sonnenberg, J. L.; Hada, M.; Ehara, M.; Toyota, K.; Fukuda, R.; Hasegawa, J.; Ishida, M.; Nakajima, T.; Honda, Y.; Kitao, O.; Nakai, H.; Vreven, T.; Montgomery, J. A., Jr.; Peralta, J. E.; Ogliaro, F.; Bearpark, M.; Heyd, J. J.; Brothers, E.; Kudin, K. N.; Staroverov, V. N.; Kobayashi, R.; Normand, J.; Raghavachari, K.; Rendell, A.; Burant, J. C.; Iyengar, S. S.; Tomasi, J.; Cossi, M.; Rega, N.; Millam, N. J.; Klene, M.; Knox, J. E.; Cross, J. B.; Bakken, V.; Adamo, C.; Jaramillo, J.; Gomperts, R.; Stratmann, R. E.; Yazyev, O.; Austin, A. J.; Cammi, R.; Pomelli, C.; Ochterski, J. W.; Martin, R. L.; Morokuma, K.; Zakrzewski, V. G.; Voth, G. A.; Salvador, P.; Dannenberg, J. J.; Dapprich, S.; Daniels, A. D.; Farkas, Ö.; Foresman, J. B.; Ortiz, J. V.; Cioslowski, J.; Fox, D. J. Gaussian, Inc., Wallingford CT, 2009.
- 28 M. A. Teruel, S. I. Lane, A. Mellouki, G. Solignac, G. Le Bras, Atmos. Env., 2006, **403**, 764–3772.
- 29 M. B. Blanco, M. A. Teruel, J. Phys. Org. Chem, 2008, **21**, 397–401.
- 30 I. Smith, A. R. Ravishankara. J. Phys. Chem. A, 2002, **106**, 4798–4807.
- 31 M.B. Blanco, I. Barnes, P. Wiesen. J. Phys. Chem. A, 2012, **116**, 6033–6040.
- 32 A. Mellouki, G. Le Bras, H. Sidebottom. Chem. Rev., 2003, **103**, 5077–5096.
- 33 S. Xu, M. C. Lin, Proc. Combust. Inst., 2007, **31**, 159–166.34 L. Y. Yeung, M. J. Pennino, A. M. Miller, M. J. Elrod, J. Phys. Chem. A, 2005, **109**, 1879–1889.
- 34 A. Mellouki, T. J. Wallington, J. Chen, Chem. Rev., 2015, **115**, 3984–4014.
- 35 R. J. Cvetanović, D. L. Singleton, Rev. Chem. Intermed., 1984, **5**, 183–226.
- 36 R. Atkinson, J. Arey. Chem. Rev., 2003, **103**, 4605–4638.
- 37 D. L. Singleton, R. J. Cvetanović, J. Am. Chem. Soc., 1976, **98**, 6812–6819.
- 38 R. Atkinson. Chem. Rev., 1986, **86**, 69–201.
- 39 J. R. Alvarez-Idaboy, N. Mora-Diez, A. Vivier-Bunge, J. Am. Chem. Soc., 2000, **122**, 3715–3720.

*2-Propin-1-ol**Propyne*

$$k_1 = (2.05 \pm 0.30) \times 10^{-11} \text{ cm}^3 \text{ molecule}^{-1} \text{ s}^{-1}$$



Experimental
determination

Theoretical comparison
(OH_{addition} VS. -H_{Abstraction})



$$k_1 > k_2$$



1 atm
298K